Methane emissions responsible for record-breaking atmospheric methane growth rates in 2020 and 2021

Liang Feng[1], Paul I. Palmer[1,2,*], Robert J. Parker[3,4], Mark F. Lunt[2], Hartmut Bösch[3,4]

1 National Centre for Earth Observation, University of Edinburgh, Edinburgh, UK

2 School of GeoSciences, University of Edinburgh, Edinburgh, UK

3 National Centre for Earth Observation, Space Park Leicester, University of Leicester, UK

4 Earth Observation Science, School of Physics and Astronomy, University of Leicester, UK

Correspondence to: Paul I. Palmer (paul.palmer@ed.ac.uk)

Abstract. The global atmospheric methane growth rates reported by NOAA for 2020 and 2021 are the largest since systematic measurements began in 1983. To explore the underlying reasons for these anomalous growth rates we use newly available methane data from the Japanese Greenhouse gases Observing SATellite (GOSAT) to estimate methane surface emissions. Relative to baseline values in 2019 we see the largest annual increases in methane emissions during 2020 over Eastern Africa (13 Tg), tropical Asia (4 Tg), tropical South America (3 Tg), and temperate Eurasia (3 Tg), and the largest reductions over China (-6 Tg) and India (-2 Tg). We find comparable emission changes in 2021, relative to 2019, except for tropical and temperate South America where emissions increased to 9 Tg and 5 Tg, respectively, and tropical Asian emissions increased to 8 Tg. The elevated contributions we saw in 2020 over the western half of Africa (-5 Tg) and Europe (-3 Tg) are substantially reduced in 2021, compared to our 2019 baseline. We find statistically significant positive correlations between anomalies of tropical methane emissions and groundwater, consistent with recent studies that have highlighted a growing role for microbial sources over the tropics. Emission reductions over India and China are expected in 2020 due to the Covid-19 shutdown but continued in 2021, which we do not currently understand. Based on a sensitivity study for which we assume a conservative 5% decrease in hydroxyl concentrations in 2020, due to reduced pollutant emissions during the Covid-19 shutdown, we find that the global increase in our *a posteriori* emissions in 2020 is ~22% lower than our control calculation. We conclude therefore that most of the observed increase in atmospheric methane during 2020 and 2021 is due to increased emissions.

1 Introduction

The atmospheric growth rate of methane in the 21st century has defied a definitive explanation: following a period of near-zero growth during 2000-2007 (Rigby et al. 2008) growth rates have accelerated, with values reported by NOAA for 2020 (15.29±0.38 ppb) and 2021 (16.94±0.38 ppb) exceeding all prior values since their records began in 1983. The underlying reasons for these anomalous growth rates in 2020 and 2021 are currently subject to intense debate with some studies attributing

most of the growth in 2020 to a reduction in the hydroxyl radical (OH) sink of methane due to global-scale reductions in nitrogen oxides due to pandemic-related industry shutdowns (Laughner et al. 2021). On the face of it, this appears to be a reasonable explanation, but recent studies have used satellite observations of atmospheric methane to reveal regional hotspots over the tropics that are responding to changes in climate and have global significance (Pandey et al. 2021; Lunt et al. 2019;

35   2021; Pandey et al. 2017; Feng et al. 2022; Palmer et al. 2021; Wilson et al. 2020). Here, we use satellite observation of methane from the Japanese Greenhouse gases Observing SATellite (GOSAT) to document global and regional changes in emissions, extending a recent study (Feng et al. 2022). In the next section we describe the data and methods used to infer methane emissions. In section 3 we describe our results and conclude the study in section 4.

2 Data and Methods

40   We follow closely the methodology from a recent study (Feng et al. 2022) so that for the sake of brevity we include only details relevant to the calculations shown here.

2.1 GOSAT methane proxy data

We use version 9.0 of the proxy GOSAT $XCH_4:XCO_2$ retrievals (X denotes atmospheric column-averaged dry-air mole fraction) from the University of Leicester (R. J. Parker et al. 2020; R. Parker and Boesch 2020), including both nadir

45   observations over land and glint observations over the ocean. Analyses have shown that these retrievals have a bias of 0.2%, with a single-sounding precision of ~0.72%. We globally remove a slightly larger 0.3% bias from the GOSAT proxy data to improve the comparison with independent *in situ* observations. We assume that each single GOSAT proxy $XCH_4:XCO_2$ ratio retrieval has an uncertainty of 1.2% to account for possible model errors, including the errors in atmospheric chemistry and transport.

50   ### 2.2 *In situ* data

To anchor the GOSAT proxy ratio observations (Fraser et al. 2014b), we also ingest simultaneously the CO_2 and methane mole fraction data at surface-based sites, chosen from the NOAA compilation of the multi-laboratory *in-situ* measurements (Di Sarra et al. 2021; 2022; Cox et al. 2021; 2022). We include the same subset of the surface sites used by a recent study that documented year to year variations of methane emissions during 2010-2019 (Feng et al. 2022). We assume uncertainties of

55   0.5 ppm and 8 ppb for these *in situ* observations of CO_2 and methane respectively (Feng et al. 2022).

2.3 GEOS-Chem atmospheric chemistry transport model

We use the GEOS-Chem model of atmospheric chemistry and transport at a horizontal resolution of 2° (latitude) × 2.5° (longitude), driven by the MERRA2 meteorological reanalyses from the Global Modeling and Assimilation Office Global Circulation Model based at NASA Goddard Space Flight Center. Our CO_2 and methane model calculations are described in

60   recent study (Feng et al. 2022). Our *a priori* CO_2 flux inventory includes monthly biomass burning emission (van der Werf et

al. 2017); monthly fossil fuel emissions for 2019 in the absence of more recent data (Oda and Maksyutov 2021); monthly climatological ocean fluxes (Takahashi et al. 2009); and 3-hourly terrestrial biosphere fluxes (Olsen and Randerson 2004). Our *a priori* methane fluxes from nature include monthly wetland emissions, including rice paddies (Bloom et al. 2017); monthly fire methane emissions (van der Werf et al. 2017); and termite emissions (Fung et al. 1991). We include emissions

65   from geological macroseeps (Kvenvolden and Rogers 2005; Etiope 2015). For *a priori* anthropogenic emissions we use the EDGAR v4.32 global emission inventory for 2012 (Janssens-Maenhout et al. 2019) that includes various sources related to human activities (e.g., oil and gas industry, coal mining, livestock, and waste). We use monthly 3-D fields of OH, consistent with observed values for the lifetime of methyl chloroform, from the GEOS-Chem full chemistry simulation (Mao et al. 2013; Turner et al. 2015) to describe the main oxidation sink of methane. Using pre-computed fields of OH greatly simplifies our

70   calculations. To explore the sensitivity of our methane emission estimates for 2020 due to inferred reductions in OH due to large-scale industrial shutdown due to Covid-19 (Cooper et al. 2022), we scale down our baseline monthly 3-D OH fields by 5% where combustion emissions of CO_2 (Oda and Maksyutov 2021) were larger than the mean emissions over Africa, resulting in reductions mainly between 15°N and 65°N. Our choice of 5% represents a conservative reduction based on a recent study (Laughner et al. 2021). We also include the net microbial consumption of methane in soils (Fung et al. 1991), and reaction

75   with chlorine atoms (Thanwerdas et al. 2019).

2.4 Ensemble Kalman filter inverse method

We use an ensemble Kalman Filter (EnKF) framework to estimate simultaneously CO_2 and methane fluxes from satellite measurements of the atmospheric CO_2 and methane (Feng et al. 2022). Our state vector includes monthly scaling factors for 487 regional pulse-like basis functions (Figure A1) that describe CO_2 and methane fluxes, including 476 land regions and 11

80   oceanic regions. We define these land sub-regions by dividing the 11 TransCom–3 land regions into 42 nearly equal sub-regions, with the exception for temperate Eurasia that has been divided into 56 sub-regions due to its large landmass. We use the 11 oceanic regions defined by the TransCom–3 experiment. We use a 4-month moving lag window to reduce the computational costs for projecting the flux perturbation ensemble into observation space long after (>4 months) their emissions, beyond which time it is difficult to distinguish between the emitted signal from variations in the ambient background

85   atmosphere (Fraser et al. 2014a; Feng et al. 2017). Our *a priori* fluxes are described above. For simplicity we assume a fixed uncertainty of 40% for coefficients corresponding to the *a priori* CO_2 fluxes over each sub-region, and a larger uncertainty (60%) for the corresponding methane emissions. We also assume that *a priori* errors for the same gas are correlated with a spatial correlation length of 300 km and with a temporal correlation of one month.

90   As a sensitivity test, we also report methane fluxes inferred using the same EnKF approach but using the proxy GOSAT XCH4 data. These GOSAT XCH4 retrievals are calculated from the XCH4:XCO2 ratio by applying an ensemble mean of model XCO2, and then bias-corrected according to comparison with TCCON XCH4 retrievals (R. J. Parker et al. 2020).

Atmospheric
Chemistry
and Physics
Discussions

2.5 Correlative data

To help interpret the changes in methane emission estimates we use additional datasets that are relevant to microbial or pyrogenic production of methane. We use monthly surface temperature fields at a spatial resolution of 2°x2.5° from the Modern-Era Retrospective Analysis for Research and Applications, version 2 (MERRA2) developed by the Global Modeling and Assimilation Office, NASA Goddard Space Flight Center (Bosilovich *et al.*, 2015). Precipitation data are taken from the NOAA CMAP (CPC Merged Analysis of Precipitation) long-term global rainfall dataset (Xie and Arkin 1997) that provides near-global monthly coverage at a spatial resolution of 2.5° × 2.5°, from 1979 to near-present. In addition, we use monthly total water storage (liquid water equivalent depth, LWE) on a 1° × 1° global grid from the NASA/DLR Gravity Recovery and Climate Experiment Follow-on (GRACE-FO) (Landerer et al. 2020). Finally, we explore monthly biomass burning emissions from the Global Fire Emissions Database (GFED v4) (van der Werf et al. 2017).

2 Results

Table 1 summarizes our global emission estimates inferred from GOSAT for 2020 and 2021; and for 2019, which we use as our baseline year throughout this study (Figure A2). The largest change in our global *a posteriori* emissions occurs during 2019—2020 (27 Tg) from 583.7 to 610.7 Tg/yr. Our *a posteriori* emission estimates for 2019 and 2020 are within 2% of values reported by an independent study (Qu et al, *Attribution of the 2020 surge in atmospheric methane by inverse analysis of GOSAT observations*, submitted to ERL, 2022, available from their group website https://acmg.seas.harvard.edu/publications-acmg; hereinafter denoted as Qu et al, 2022), consistent with our reported uncertainties. These elevated emissions are sustained, but not further increased, during 2021 (609.5 Tg/yr).

The 27 Tg emission increase in 2020 and the lack of further emissions growth in 2021 may appear inconsistent with the NOAA global annual mean growth rates of 15.3 and 16.9 ppb in 2020 and 2021, respectively (Table 1). Based on these reported atmospheric growth rates, and after considering the effects of methane sinks, we find that a one-box model calculation predicts an increase in emissions of 12.6 Tg between 2019 and 2020 and a further 15.1 Tg increase in 2021 (see Appendix B and Figure B1). These calculations use annual mean values that effectively represent the emissions increase between the middle of each successive year rather than the beginning and end. After considering the increases in monthly mean NOAA data, we find that the simple box model predicts a similar increase in emissions between December 2019 (583 Tg yr^{-1}) and December 2020 (610 Tg yr^{-1}) of 27 Tg yr^{-1}, with emissions thereafter stabilizing, with mean emissions of 610 Tg yr^{-1} in 2021. As such, we conclude that the global mean emission results inferred from GOSAT are consistent with those inferred from NOAA surface data, assuming a fixed methane atmospheric lifetime.

Figure 1 shows the broad geographical breakdown for our reported global changes in methane emissions. Relative to 2019, we find widespread increased emissions during 2020 except for China and India. Relative to baseline values in 2019 we see the

Atmospheric
Chemistry
and Physics
Discussions

5-1

5-2

125   largest annual increases in methane emissions during 2020 over Eastern Africa (13 Tg), tropical Asia (4 Tg), tropical South

America (3 Tg), and temperate Eurasia (3 Tg), and the largest reductions over China (-6 Tg) and India (-2 Tg). Emission

changes relative to 2019 are comparable in 2021, except for tropical and temperate South America increases to 9 Tg and 5 Tg,

respectively, and tropical Asia increases to 8 Tg. The elevated contributions we saw in 2020 over the western half of Africa

(-5 Tg) and Europe (-3 Tg) are substantially reduced in 2021, compared to our 2019 baseline.

130

Figure 2 shows the distribution of methane emissions from 2020 and 2021 and the relative changes from 2019 (Figure A1).

During 2020, there are significant decreases (20-30%) over the manufacturing regions such as eastern China, India, central

America, and eastern Europe. There are also significant increases across eastern Africa (30-40%), eastern North America

(30%), and maritime Southeast Asia (30%). During 2021, we see similar changes in emissions, but they are typically

135   exaggerated. There is more of a pronounced increase over East Africa (>50%), southern Brazil (50%), and eastern North

America (up to 40%), and large decreases over eastern China (-50%) and western Russia (-50%). During 2021 there is also a

large decrease over equatorial West Africa and eastern Europe (Figure 1). There are substantial seasonal changes in methane

emissions (Figure A3) that are broadly consistent with seasonal changes in temperature and rainfall (not shown).

140   Figure 3 shows different annual surface temperature warming patterns in 2020 and 2021. During 2020 the high northern

latitudes are dominated by summer warming over Siberia (2-3 K on an annual scale) that has been linked to greenhouse gas

emissions (Ciavarella et al. 2021) and surface temperatures over Alaska were 2-3 K cooler than baseline values in 2019, where

5-3   there were comparatively small changes in groundwater (< 5 cm). North America, western Europe and Scandinavia also

experienced anomalously warm annual mean temperatures (typically within ±2 K of 2019 values). There were smaller changes

145   in temperatures at low latitudes (typically ±1 K of 2019 values), but larger increases in groundwater (±10-20 cm) associated

with higher changes in rainfall (Figure A4), particularly over East Africa and eastern Brazil. During 2021, high northern

latitudes were cooler than 2019 (<2-3 K) except for the contiguous US and Canada (higher than 2019 values by 2-3 K).

Midlatitudes and low latitudes generally did not experience the warm temperatures of 2020. Elevated groundwater was

sustained in 2021 over East and Southern Africa, eastern tropical South America (principally Brazil but stretching up to

150   Venezuela), central America, India, maritime Southeast Asia, and north and southeast Australia. Groundwater decreased over

the contiguous US, part of tropical South America and parts of Eurasia. We find generally stronger annual and seasonal

relationships between methane emission anomalies and hydrological anomalies (rainfall and groundwater) for 2020 and 2021

than for temperature anomalies. Particularly, we find statistically significant large-scale positive correlations (typically 0.5-   5-4

0.6; p<0.001) for all seasons between methane and groundwater anomalies over Eastern Africa, tropical South America, and

155   tropical Asia, but no significant correlation between methane and surface temperature anomalies. This is consistent with recent

studies that have highlighted an increasing role for microbial sources in the tropical methane budget (Lunt et al. 2019; Feng et

al. 2022; Wilson et al. 2020). Over North America, we find a significant negative correlation (from -0.3 to -0.5; p<0.001) with

rainfall during MAM and JJA and a significant positive correlation with temperature during JJA (0.3; p < 0.001), which we do

Atmospheric
Chemistry
and Physics
Discussions

not currently understand. Fire emissions did not increase much where we report the largest increases in methane emissions in

160   2020 or 2021, except over central Canadian provinces. (Figure A4).

To explore the robustness of our results, we explore two sensitivity runs. First, we ran our inversion for 2020 with OH concentrations decreased by 5% over regions with large anthropogenic emissions (as described in section 2.3), a conservative estimate for the value we expect based on widespread reductions in nitrogen oxide emissions due to shutting manufacturing

165   and other industries during Covid-19 lockdowns (Laughner et al. 2021). A reduction in OH, assuming constant emissions, would lead to an increase in atmospheric methane. Ignoring that possibility would result in a positive bias for reported methane emissions estimates. We find that our imposed 5% decrease in OH concentrations results in an emission reduction of 6.0 Tg/yr, representing 22% of the emission increase, relative to 2019, in the control run. Figure 4 show that the largest impacts of reducing OH on *a posteriori* methane emissions are of the order of ±10% over regions where there are the largest decreases in

170   nitrogen oxide emissions (Cooper et al. 2022), including China, India, Europe, North America. The regions where values are higher than the control are a consequence of mass balance. Our conservative 5% OH decrease cannot fully explain the increase in atmospheric methane, and consequently regions where OH were not decreased have had to compensate. The results for a smaller 1% decrease in OH have similar distributions but smaller changes (not shown). Second, we ran an experiment in which we used the methane columns determined by the proxy data, assuming model values for CO_2 (R. J. Parker et al. 2020). Using

175   these data, we find our results for 2020 and 2021 are within a few percent of the values we report using the proxy data directly (Figure A5). Both sensitivity experiments provide confidence in our emission estimates and that most of the atmospheric methane growth in 2020 was due to an increase in emissions.

3 Concluding Remarks

180   We reported regional emission estimates of methane during 2020 and 2021, two years with record-breaking atmospheric growth rates, inferred from satellite observations of methane from the Japanese Greenhouse gases Observing SATellite.

We find in both years that emissions from Eastern Africa, tropical Asia, and tropical South America dominate the global atmospheric growth rate, increasing by 11-13 Tg/yr, 4-8 Tg/yr, and 3-9 Tg relative to the 2019 baseline year, respectively.

185   During 2020, we also find substantial increased emissions, relative to the 2019 baseline values, from Australia (3 Tg) and temperate Eurasia (3 Tg). Emission changes relative to 2019 are comparable in 2021, except for temperate South America that increases to 5 Tg and temperate North America that increases to 3 Tg. The elevated contributions we saw in 2020 over the western half of Africa (-5 Tg) and Europe (-3 Tg) are substantially reduced in 2021, compared to our 2019 baseline. We find statistically significant positive correlations between tropical methane emission and hydrological anomalies, consistent with

190   recent studies that have highlighted a growing role for microbial sources over the tropics (Lunt et al. 2019; Feng et al. 2022;

Wilson et al. 2020). Our results are broadly consistent with a recent study of the 2020 period (Qu et al, 2022), including the magnitude of change associated with a change in OH, albeit concluded using an independent method.

195   Substantial, widespread reductions in nitrogen oxides during 2020 associated with the shutdown of manufacturing and other industries will have perturbed atmospheric concentrations of the OH loss of methane. A reduction in OH could also help explain, in principle, the record-breaking atmospheric increase in methane. Here we explore that issue by scaling back our prescribed OH fields by 5% over fossil fuel combustion regions to assess the impact of our reported increases in methane emissions. We find a 5% decrease in OH results in an *a posteriori* emission reduction of 6.0 Tg compared to our control run that does not consider a decrease in OH, equivalent to 22% of the emission increase in our control run for 2020. These changes

200   are mainly focused over fossil fuel emitting regions, as expected. This result suggests that an increase in emissions was predominately responsible for the observed growth in atmospheric methane during 2020.

7-1

This study highlights the tremendous value of using satellite observations to understand rapid changes in atmospheric methane. They provide crucial information not only to identify regional column hotspots associated with emissions but also provide

205   correlative information to help attribute those hotspots to specific anthropogenic or natural emissions.

Data availability. The University of Leicester GOSAT Proxy v9.0 XCH$_4$ data are available from the Centre for Environmental Data Analysis data repository at https://doi.org/10.5285/18ef8247f52a4cb6a14013f8235cc1eb. Precipitation, temperature, and the GRACE datasets are available at http://grace.jpl.nasa.gov. The community-led GEOS-Chem model of atmospheric

210   chemistry and model is maintained centrally by Harvard University (http://geos-chem.seas.harvard.edu), and is available on request. The ensemble Kalman filter code is publicly available as PyOSSE (https://www.nceo.ac.uk/data-tools/atmospheric-tools/).

Author contributions. LF and PIP designed the research; LF and MFL prepared the calculations; RJP and HB provided the

215   GOSAT data and expert advice on its usage; PIP wrote the paper, with comments from LF, RJP, MFL, and HB.

Competing interests. The contact author has declared that neither they nor their co-authors have any competing interests.

Atmospheric
Chemistry
and Physics
Discussions

Package (ObsPack) data products, coordinated by NOAA ESRL, and making them freely available for carbon cycle research. We also thank the GEOS-Chem community, particularly the team at Harvard University who help maintain the GEOS-Chem model, and the NASA Global Modeling and Assimilation Office (GMAO) who provide the MERRA2 data product.

References

Bloom, A A, K W Bowman, M Lee, A J Turner, R Schroeder, J R Worden, R Weidner, K C McDonald, and D J Jacob. 2017. "A Global Wetland Methane Emissions and Uncertainty Dataset for Atmospheric Chemical Transport Models (WetCHARTs Version 1.0)." *Geoscientific Model Development* 10 (6): 2141–56. https://doi.org/10.5194/gmd-10-2141-2017.

Bosilovich, M. G, S Akella, L Coy, R Cullather, C Draper, R Gelaro, R Kovach, et al. 2015. "MERRA-2: Initial Evaluation of the Climate."

Ciavarella, Andrew, Daniel Cotterill, Peter Stott, Sarah Kew, Sjoukje Philip, Geert Jan van Oldenborgh, Amalie Skålevåg, et al. 2021. "Prolonged Siberian Heat of 2020 Almost Impossible without Human Influence." *Climatic Change* 166 (1): 9.

Cooper, Matthew J., Randall V. Martin, Melanie S. Hammer, Pieternel F. Levelt, Pepijn Veefkind, Lok N. Lamsal, Nickolay A. Krotkov, Jeffrey R. Brook, and Chris A. McLinden. 2022. "Global Fine-Scale Changes in Ambient NO_2 during COVID-19 Lockdowns." *Nature* 601 (7893). https://doi.org/10.1038/s41586-021-04229-0.

Cox, Adam, Alcide Giorgio Di Sarra, Anna Karion, Arlyn Andrews, Aurelie Colomb, Bert Scheeren, Bill Paplawsky, et al. 2022. "Multi-Laboratory Compilation of Atmospheric Carbon Dioxide Data for the Year 2021; Obspack_co2_1_NRT_v7.1_2022-03-04." NOAA Earth System Research Laboratory, Global Monitoring Laboratory. https://doi.org/10.25925/20220301.

Cox, Adam, Alcide Giorgio Di Sarra, Alex Vermeulen, Alistair Manning, Andreas Beyersdorf, Andreas Zahn, Andrew Manning, et al. 2021. "Multi-Laboratory Compilation of Atmospheric Carbon Dioxide Data for the Period 1957-2020; Obspack_co2_1_GLOBALVIEWplus_v7.0_2021-08-18." NOAA Global Monitoring Laboratory. https://doi.org/10.25925/20210801.

Etiope, E. 2015. *Natural Gas Seepage: The Earth's Hydrocarbon Degassing*. Springer.

Feng, L., Paul I Palmer, Hartmut Bösch, Robert J Parker, Alex J Webb, Caio S C Correia, Nicholas M Deutscher, et al. 2017. "Consistent Regional Fluxes of CH_4 and CO_2 Inferred from GOSAT Proxy XCH_4: XCO_2 Retrievals, 2010--2014." *Atmos. Chem. Phys* 17: 4781–97.

255 Feng, L., Paul I Palmer, Sihong Zhu, Robert J Parker, and Yi Liu. 2022. "Tropical Methane Emissions Explain Large Fraction of Recent Changes in Global Atmospheric Methane Growth Rate." *Nature Communications* 13 (1): 1378. https://doi.org/10.1038/s41467-022-28989-z.

Fraser, A., P. I. Palmer, L. Feng, H. Bösch, R. Parker, E. J. Dlugokencky, P. B. Krummel, and R. L. Langenfelds. 2014a. "Estimating Regional Fluxes of CO_2 and CH_4 Using Space-Borne Observations of XCH_4: XCO_2." *Atmospheric*
260 *Chemistry and Physics* 14 (23). https://doi.org/10.5194/acp-14-12883-2014.

Fraser, A, P I Palmer, L Feng, H Bösch, R Parker, E J Dlugokencky, P B Krummel, and R L Langenfelds. 2014b. "Estimating Regional Fluxes of CO_2 and CH_4 Using Space-Borne Observations of XCH_4: XCO_2." *Atmospheric Chemistry and Physics* 14 (23): 12883–95. https://doi.org/10.5194/acp-14-12883-2014[FL1].

Fung, I, J John, J Lerner, E Matthews, M Prather, L P Steele, and P J Fraser. 1991. "Three-Dimensional Model Synthesis of
265 the Global Methane Cycle." *Journal of Geophysical Research: Atmospheres* 96 (D7): 13033–65. https://doi.org/https://doi.org/10.1029/91JD01247.

Gurney, Kevin Robert, Rachel M Law, A Scott Denning, Peter J Rayner, Bernard C Pak, David Baker, Philippe Bousquet, et al. 2004. "Transcom 3 Inversion Intercomparison: Model Mean Results for the Estimation of Seasonal Carbon Sources and Sinks." *Global Biogeochemical Cycles* 18 (1).

270 Janssens-Maenhout, G, M Crippa, D Guizzardi, M Muntean, E Schaaf, F Dentener, P Bergamaschi, et al. 2019. "EDGAR v4.3.2 Global Atlas of the Three Major Greenhouse Gas Emissions for the Period 1970--2012." *Earth System Science Data* 11 (3): 959–1002. https://doi.org/10.5194/essd-11-959-2019.

Kvenvolden, K A, and B W Rogers. 2005. "Gaia's Breath's Global Methane Exhalations." *Marine and Petroleum Geology* 22 (4): 579–90. https://doi.org/https://doi.org/10.1016/j.marpetgeo.2004.08.004.

275 Landerer, Felix W, Frank M Flechtner, Himanshu Save, Frank H Webb, Tamara Bandikova, William I Bertiger, Srinivas V Bettadpur, et al. 2020. "Extending the Global Mass Change Data Record: {GRACE} Follow-On Instrument and Science Data Performance." *Geophysical Research Letters* 47 (12). https://doi.org/10.1029/2020gl088306.

Laughner, Joshua L., Jessica L. Neu, David Schimel, Paul O. Wennberg, Kelley Barsanti, Kevin W. Bowman, Abhishek Chatterjee, et al. 2021. "Societal Shifts Due to COVID-19 Reveal Large-Scale Complexities and Feedbacks between
280 Atmospheric Chemistry and Climate Change." *Proceedings of the National Academy of Sciences of the United States of America* 118 (46). https://doi.org/10.1073/pnas.2109481118.

Lunt, M. F., P I Palmer, L Feng, C M Taylor, H Boesch, and R J Parker. 2019. "An Increase in Methane Emissions from Tropical Africa between 2010 and 2016 Inferred from Satellite Data." *Atmos. Chem. Phys.* 19 (23): 14721–40. https://doi.org/10.5194/acp-19-14721-2019.

285 Lunt, M F, P I Palmer, A Lorente, T Borsdorff, J Landgraf, R J Parker, and H Boesch. 2021. "Rain-Fed Pulses of Methane from East Africa during 2018-2019 Contributed to Atmospheric Growth Rate." *Environmental Research Letters* 16 (2): 24021. https://doi.org/10.1088/1748-9326/abd8fa.

Mao, Jingqiu, Fabien Paulot, Daniel J Jacob, Ronald C Cohen, John D Crounse, Paul O Wennberg, Christoph A Keller, Rynda

Atmospheric
Chemistry
and Physics
Discussions

C Hudman, Michael P Barkley, and Larry W Horowitz. 2013. "Ozone and Organic Nitrates over the Eastern United States: Sensitivity to Isoprene Chemistry." *Journal of Geophysical Research: Atmospheres* 118 (19): 11,211-256,268. https://doi.org/https://doi.org/10.1002/jgrd.50817.

Oda, T, and S Maksyutov. 2021. "ODIAC Fossil Fuel CO_2 Emissions Dataset (Version Name: ODIAC2020b)." Center for Global Environmental Research, National Institute for Environmental Studies. https://doi.org/10.17595/20170411.001.

Olsen, Seth C., and James T. Randerson. 2004. "Differences between Surface and Column Atmospheric CO_2 and Implications for Carbon Cycle Research." *Journal of Geophysical Research: Atmospheres* 109 (2). https://doi.org/10.1029/2003jd003968.

Palmer, P I, L Feng, M F Lunt, R J Parker, H Bösch, X Lan, L Alba, and B Tobiaa. 2021. "The Added Value of Satellite Observations of Methane for Understanding the Contemporary Methane Budget." *Phil. Trans. R. Soc. A.* 379 (20210106). https://doi.org/http://doi.org/10.1098/rsta.2021.0106.

Pandey, Sudhanshu, Sander Houweling, Maarten Krol, Ilse Aben, Guillaume Monteil, Narcisa Nechita-Banda, Edward J Dlugokencky, et al. 2017. "Enhanced Methane Emissions from Tropical Wetlands during the 2011 La Niña." *Scientific Reports* 7 (1). https://doi.org/10.1038/srep45759.

Pandey, Sudhanshu, Sander Houweling, Alba Lorente, Tobias Borsdorff, Maria Tsivlidou, A. Anthony Bloom, Benjamin Poulter, Zhen Zhang, and Ilse Aben. 2021. "Using Satellite Data to Identify the Methane Emission Controls of South Sudan's Wetlands." *Biogeosciences*. https://doi.org/10.5194/bg-18-557-2021.

Parker, R., and Hartmut Boesch. 2020. "University of Leicester GOSAT Proxy XCH4 v9.0." Centre for Environmental Data Analysis.

Parker, R J, Alex Webb, Hartmut Boesch, Peter Somkuti, Rocio Barrio Guillo, Antonio Di Noia, Nikoleta Kalaitzi, et al. 2020. "A Decade of GOSAT Proxy Satellite CH4 Observations." *Earth System Science Data* 12 (4). https://doi.org/10.5194/essd-12-3383-2020.

Rigby, M, R G Prinn, P J Fraser, P G Simmonds, R L Langenfelds, J Huang, D M Cunnold, et al. 2008. "Renewed Growth of Atmospheric Methane." *Geophysical Research Letters* 35 (22). https://doi.org/https://doi.org/10.1029/2008GL036037.

Sarra, Alcide Giorgio Di, Ankur Desai, Anna Karion, Arlyn Andrews, Aurelie Colomb, Bert Scheeren, Brian Viner, et al. 2022. "Multi-Laboratory Compilation of Atmospheric Methane Data for the Year 2021; Obspack_ch4_1_NRT_v4.0_2022-03-03." NOAA Earth System Research Laboratory, Global Monitoring Laboratory. https://doi.org/10.25925/20211101.

Sarra, Alcide Giorgio Di, Andreas Zahn, Andrew Watson, Ankur Desai, Anna Karion, Arlyn Andrews, Aurelie Colomb, et al. 2021. "Multi-Laboratory Compilation of Atmospheric Methane Data for the Period 1983-2020; Obspack_ch4_1_GLOBALVIEWplus_v4.0_2021-10-14." NOAA Global Monitoring Laboratory. https://doi.org/10.25925/20211001.

Takahashi, Taro, Stewart C Sutherland, Rik Wanninkhof, Colm Sweeney, Richard A Feely, David W Chipman, Burke Hales, et al. 2009. "Climatological Mean and Decadal Change in Surface Ocean PCO2, and Net Sea-Air CO_2 Flux over the

Global Oceans." *Deep Sea Research Part II: Topical Studies in Oceanography* 56 (8): 554–77. https://doi.org/https://doi.org/10.1016/j.dsr2.2008.12.009.

325 Thanwerdas, J, M Saunois, A Berchet, I Pison, D Hauglustaine, M Ramonet, C Crevoisier, B Baier, C Sweeney, and P Bousquet. 2019. "Impact of Atomic Chlorine on the Modelling of Total Methane and Its ^{13}C:^{12}C Isotopic Ratio at Global Scale." *Atmospheric Chemistry and Physics Discussions* 2019: 1–28. https://doi.org/10.5194/acp-2019-925.

Turner, A J, D J Jacob, K J Wecht, J D Maasakkers, E Lundgren, A E Andrews, S C Biraud, et al. 2015. "Estimating Global and North American Methane Emissions with High Spatial Resolution Using GOSAT Satellite Data." *Atmospheric*
330 *Chemistry and Physics* 15 (12): 7049–69. https://doi.org/10.5194/acp-15-7049-2015.

Werf, G R van der, J T Randerson, L Giglio, T T van Leeuwen, Y Chen, B M Rogers, M Mu, et al. 2017. "Global Fire Emissions Estimates during 1997--2016." *Earth System Science Data* 9 (2): 697–720. https://doi.org/10.5194/essd-9-697-2017.

Wilson, C, M P Chipperfield, M Gloor, R J Parker, H Boesch, J McNorton, L V Gatti, J B Miller, L S Basso, and S A Monks.
335 2020. "Large and Increasing Methane Emissions from Eastern Amazonia Derived from Satellite Data, 2010--2018." *Atmospheric Chemistry and Physics Discussions* 2020: 1–38. https://doi.org/10.5194/acp-2020-1136.

Xie, P, and P A Arkin. 1997. "'Global Precipitation: A 17-Year Monthly Analysis Based on Gauge Observations, Satellite Estimates, and Numerical Model Outputs.'" *Bulletin of the American Meteorological Society* 78 (11): 2539–58. https://doi.org/10.1175/1520-0477(1997)078<2539:GPAYMA>2.0.CO;2.

340

Figures

a

b
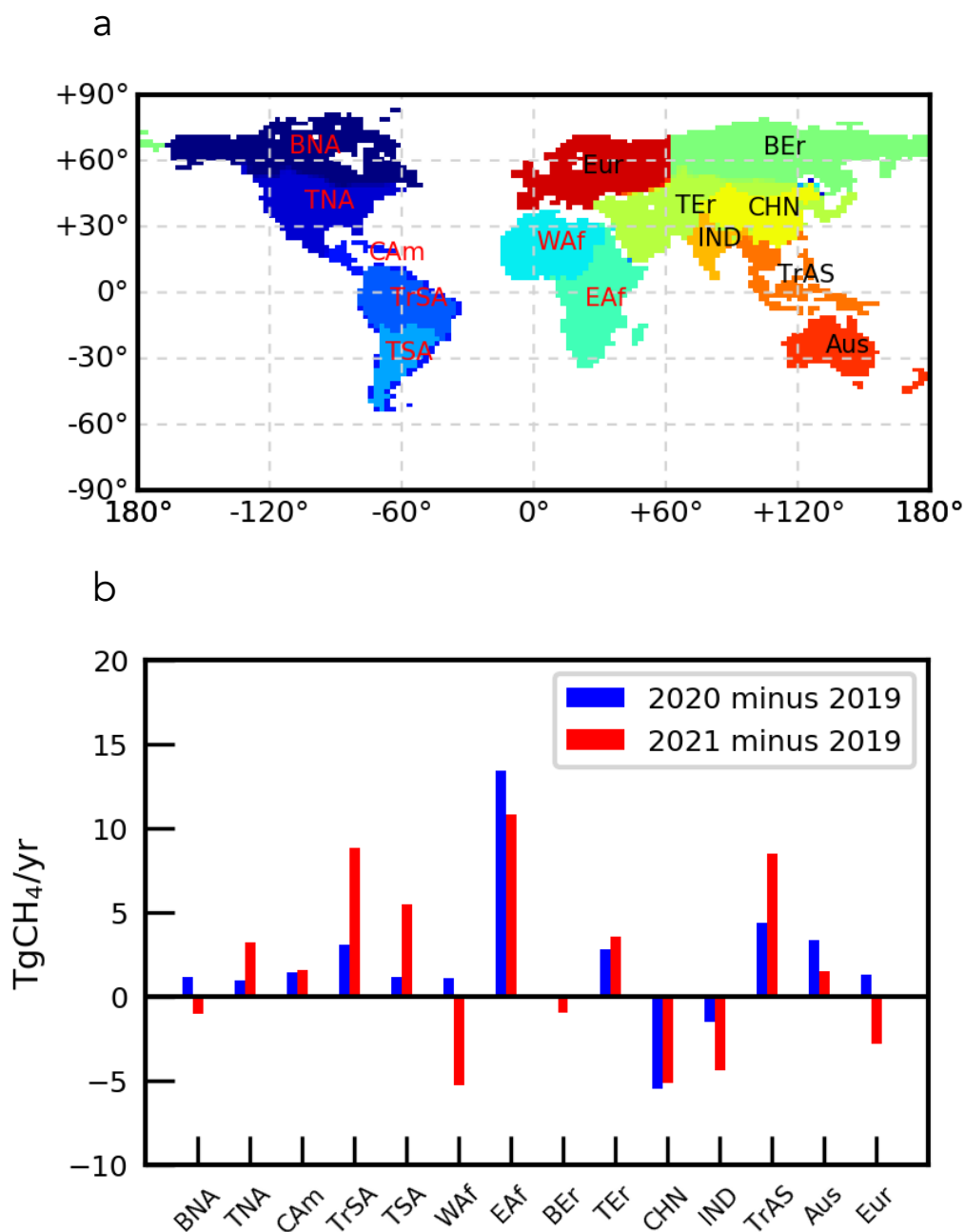
345 **Figure 1** Large-scale geographical regions a) for which we report methane changes (TgCH$_4$/yr) in 2020 and 2021 b) relative to our 2019 baseline year. Geographical regions, informed by TransCom-3 experiments (Gurney et al. 2004), include boreal North America (BNA), temperate North America (TNA), central America (Cam), tropical South America (TrSA), temperature South America (TSA), Europe (Eur), western Africa (WAf), eastern Africa (EAf), boreal Eurasia (BEr), temperate Eurasia (TEr), India (IND), China (CHN), tropical Asia (TrAs), and Australia (Aus).
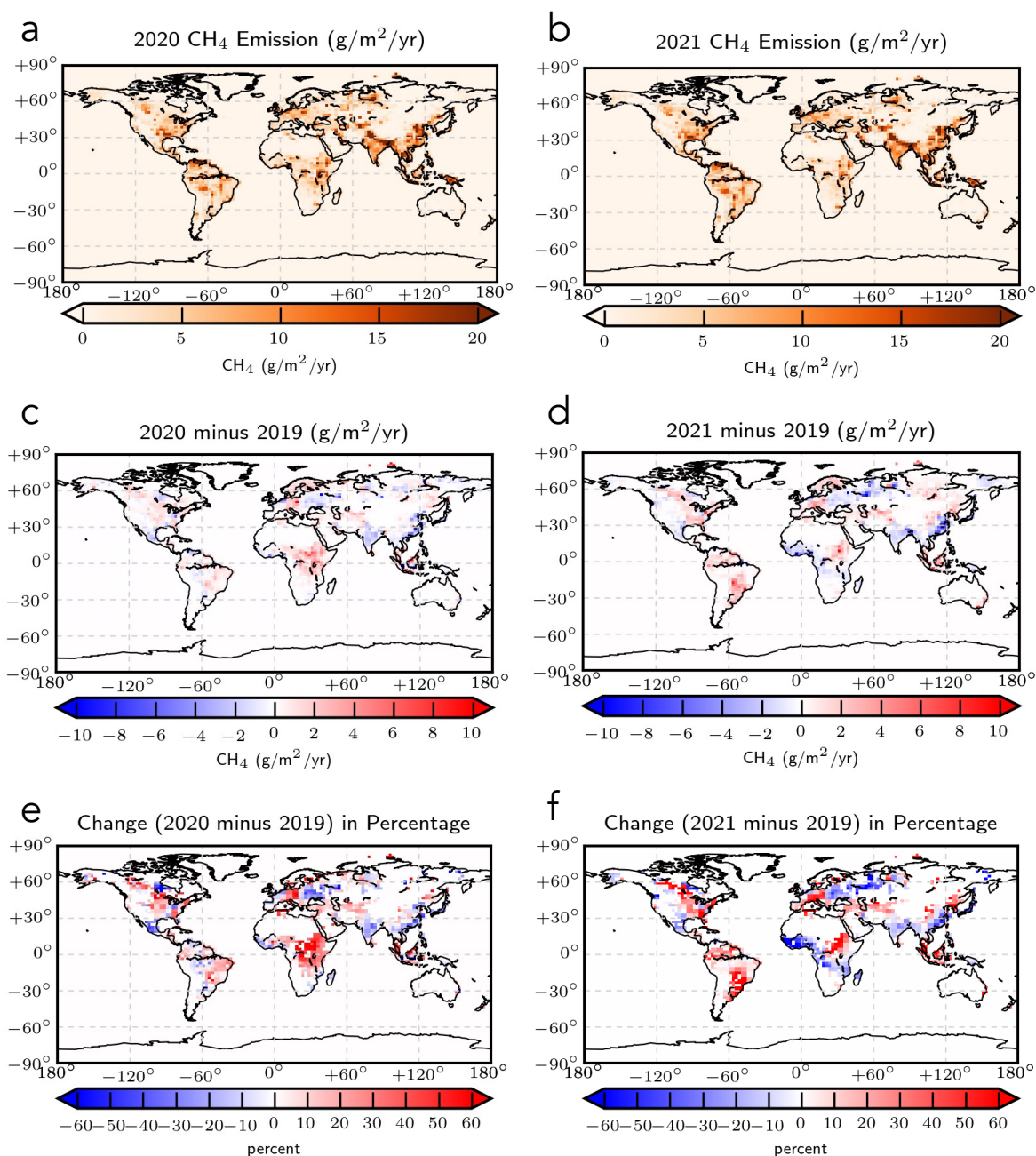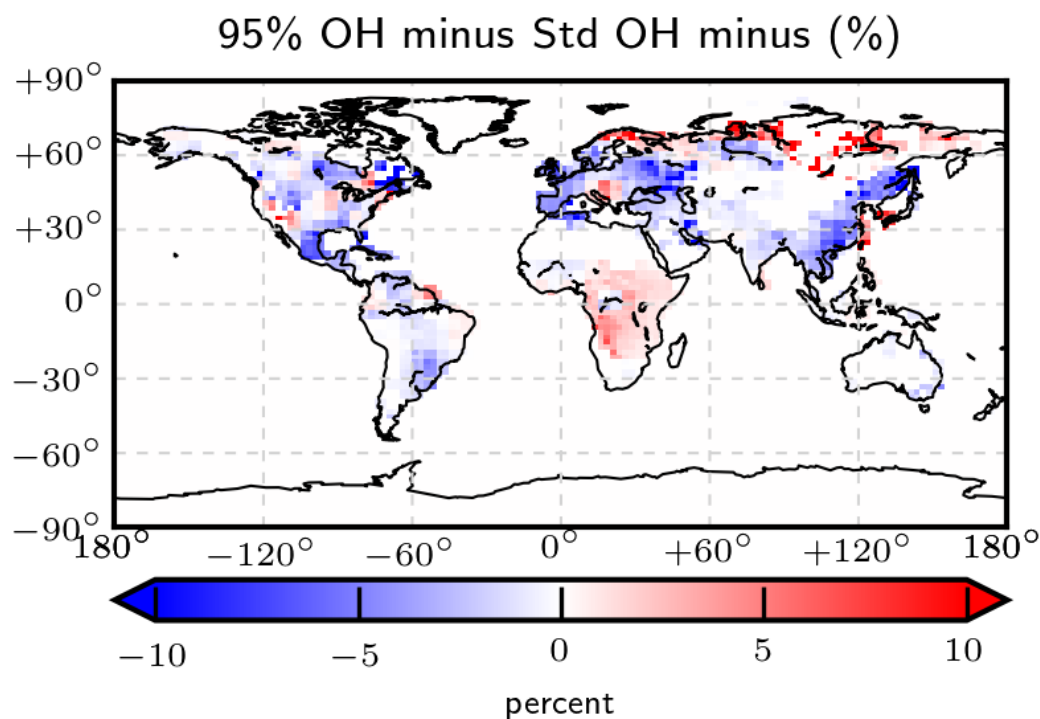
Figure 2 Global *a posteriori* emissions of methane ($g/m^2/yr$) inferred from GOSAT methane:CO_2 column ratio data for 2020 (panel a) and 2021 (panel b) and how they differ from the baseline year of 2019, described in terms of absolute (panels c and d, respectively) and percentage values (panels e and f).

Atmospheric
Chemistry
and Physics
Discussions
Open Access
EGU
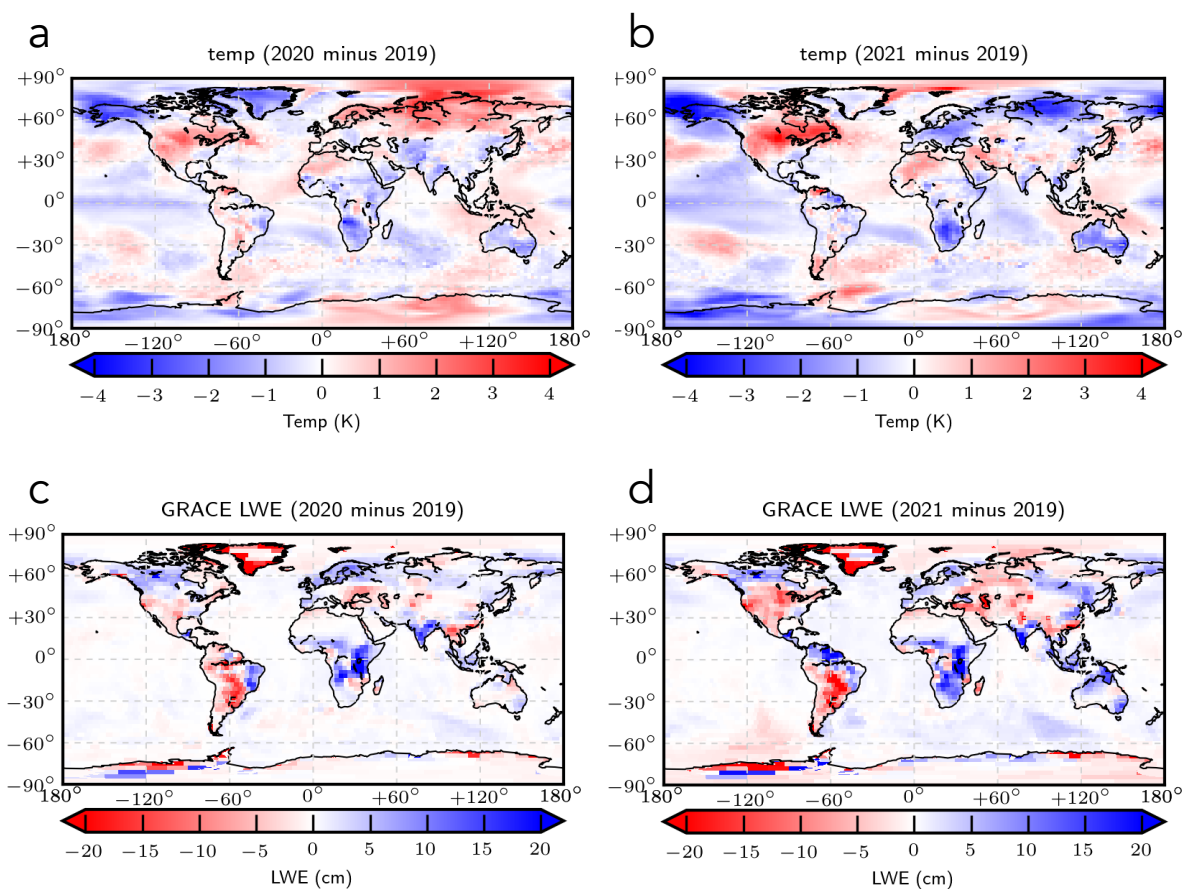
Figure 3 Global annual mean surface temperature and GRACE liquid water equivalent (LWE) anomalies in 2020 (panel a and c) and 2021 (panels b and d) relative to values in 2019.

Atmospheric
Chemistry
and Physics
Discussions

Open Access

EGU

360

Figure 4 Percentage difference in global *a posteriori* methane emissions inferred from GOSAT for 2020 between a sensitivity run in which the OH field was decreased by 5% and the control run (Figure 2).

Tables

|	Global annual methane emissions (Tg/yr)		
	2019	**2020**	**2021**
GOSAT	583.7±11.2	610.7±11.3	609.5±12.0
GOSAT with OH decreased by 5%		604.7±11.3	
In situ	588.9±18.1	601.4±18.6	--
NOAA atmospheric growth rate (ppb/yr)	9.89±0.64	15.29±0.38	16.94±0.38

365 **Table 1** Global annual emission estimates of methane (Tg/yr) inferred from GOSAT (2019-2021) and *in situ* (2019-2020) atmospheric measurements of methane. The annual atmospheric methane growth rate (ppb/yr) for 2019 to 2022 reported by NOAA is also shown.

Atmospheric
Chemistry
and Physics
Discussions

Appendix A: supplementary figures
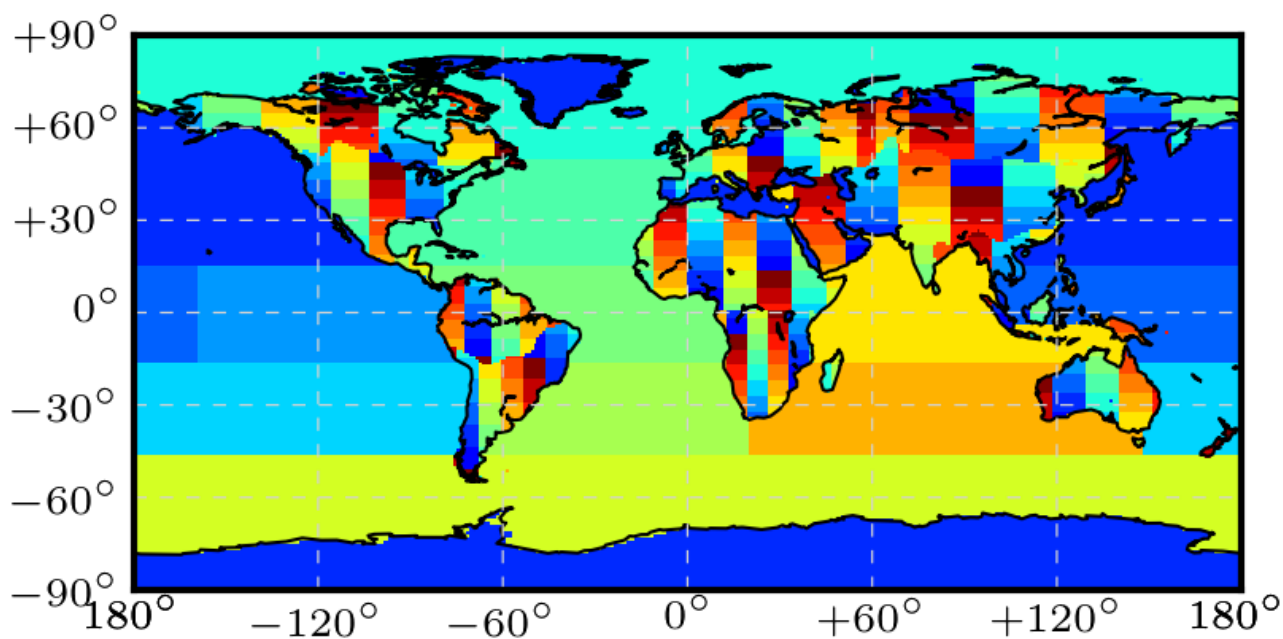
370 **Figure A1** Basis functions that describe the 487 regions where we estimate methane emissions, including 476 land regions and 11 oceanic regions.
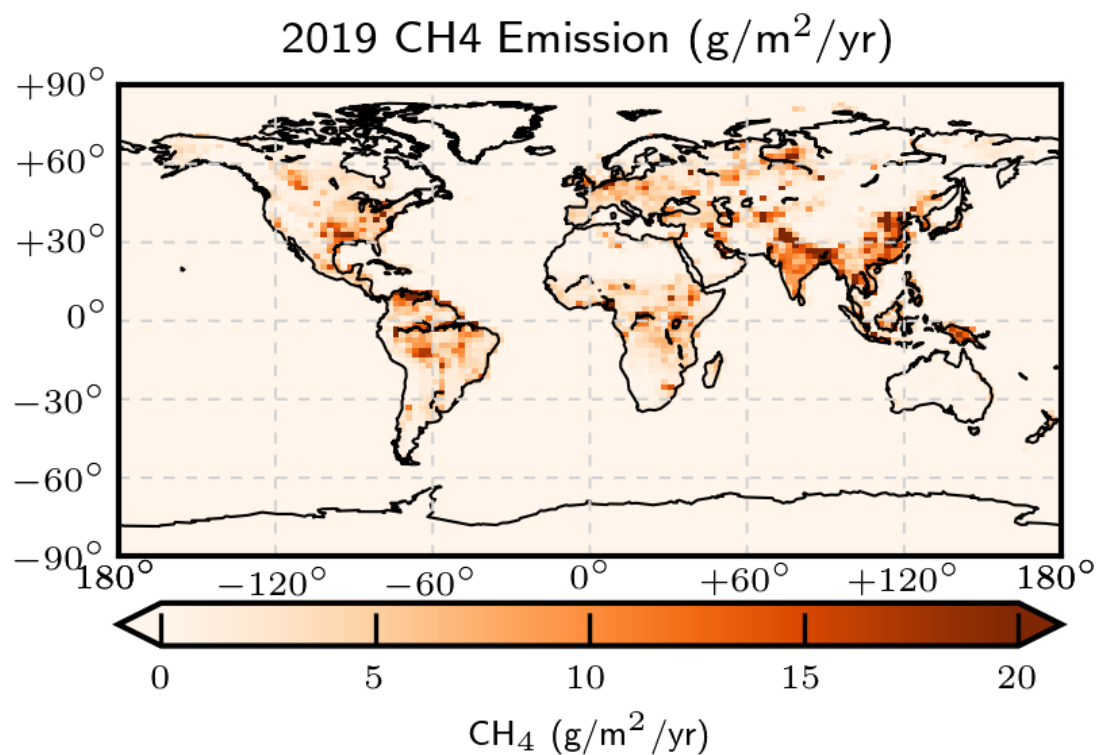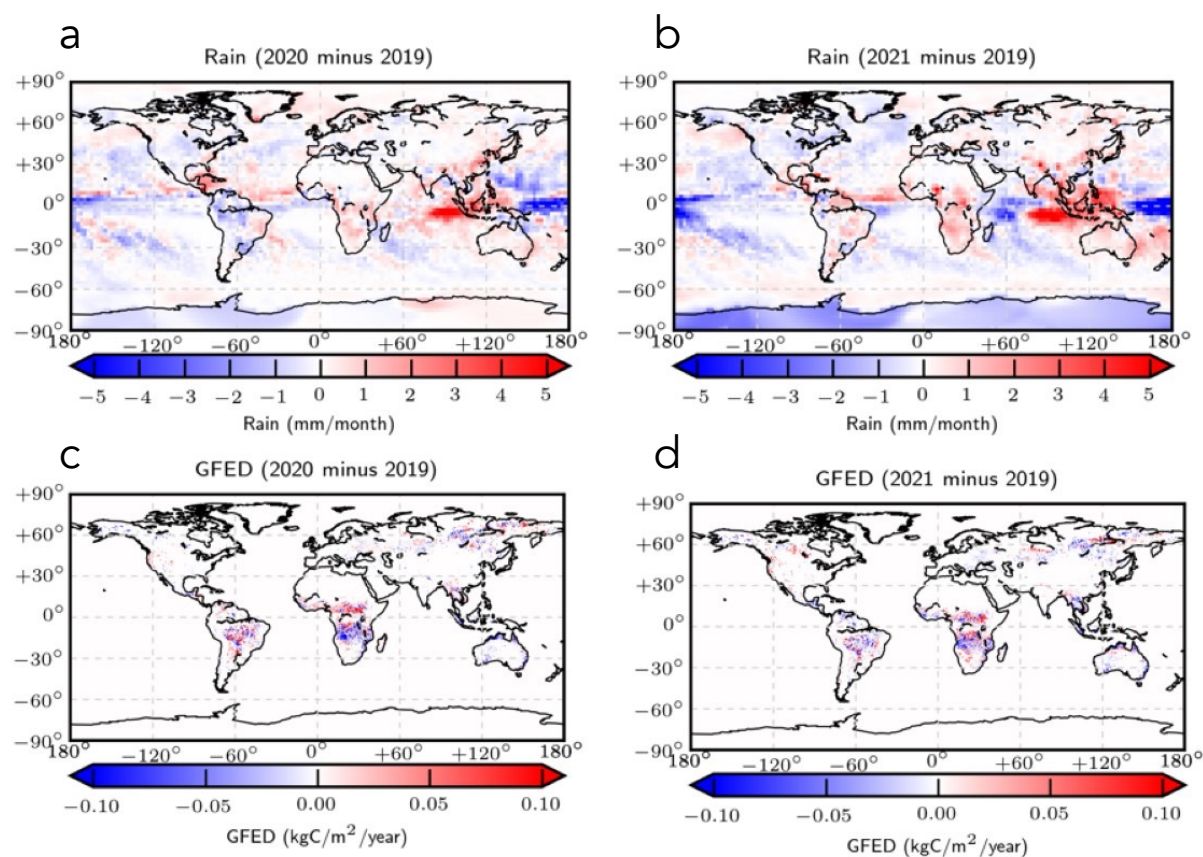
Figure A2 Global *a posteriori* emissions of methane (g/m^2/yr) inferred from GOSAT methane:CO$_2$ column ratio data for the baseline year of 2019 (Feng et al. 2022).
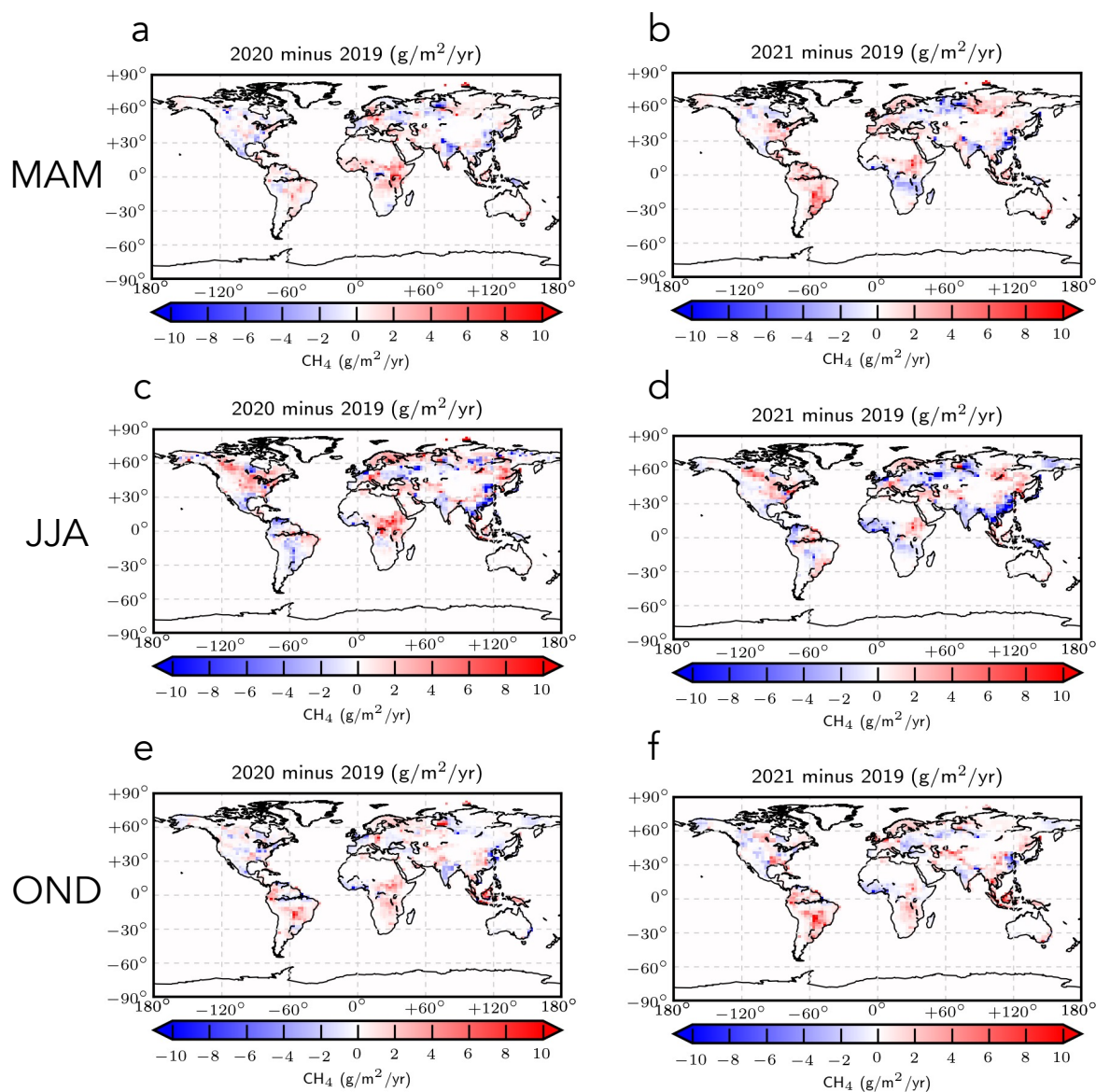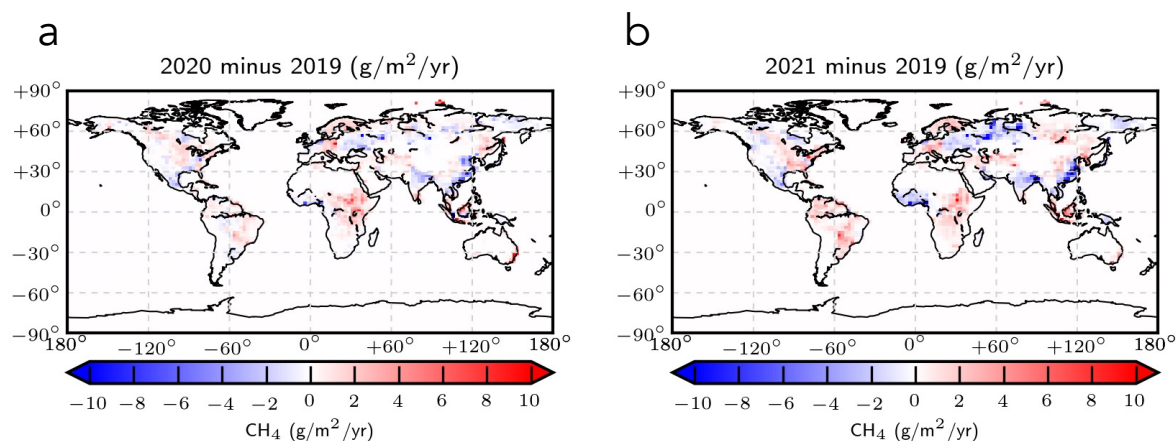
Figure A3 Global seasonal *a posteriori* emissions of methane (g/m^2/yr) inferred from GOSAT methane:CO$_2$ column ratio data for 2020 (l.h.s. panels) and 2021 (r.h.s. panels) relative to the baseline year of 2019, described in terms of absolute values. Seasons are based on rainfall changes over the tropics.

Figure A4 Global annual mean NOAA CMAP precipitation (mm/month/yr) and GFED fire emission (kgC/m²/yr) anomalies in 2020 (panel a and c) and 2021 (panels b and d) relative to values in 2019.

385

Figure A5 Global *a posteriori* emissions of methane (g/m²/yr) inferred from GOSAT methane column data for 2020 (panel a) and 2021 (panel b).

390 **Appendix B: Description of box model calculation**

To calculate global emissions of methane from the NOAA global mean data we use a simple one-box model. In this model, the change in global mean methane concentration over time is given by:

$$\frac{dB}{dt} = Q - kB$$

where B is the atmospheric mass of methane in Tg, k is the loss rate given as 1/lifetime and Q is the emissions rate. From this, after
395 integration, the annual emissions rate can be calculated as:

$$Q_t = \frac{k(B_t - B_{t-1} \cdot e^{-k})}{k(1 - e^{-k})}$$

The loss rate was tuned to match a steady state concentration of 1775 ppb during 2000-2006 based on constant emissions of 530 Tg yr^{-1} during this period. We calculated the rolling 12-month annual emissions to track the progression of global emissions between 2019 and
400 2021. We used the difference between the atmospheric concentration in January 2019 and January 2020, February 2019 to February 2020, etc. to calculate the change in emissions in the intervening 12 months. Figure B1 shows the increase in emissions throughout 2020 followed by more variable month-to-month changes in 2021. The large increase in emissions primarily occurs in 2020, with emissions at the 12-month period ending in Dec 2020 being 27 Tg yr^{-1} larger than the emissions one year earlier. In contrast if emissions are calculated using annual mean concentrations, it appears as if there is a larger emission increase in 2021. The box model results show that the highly simplified
405 calculation based on global average data is consistent with the more complex inverse modelling approach applied to the GOSAT data.
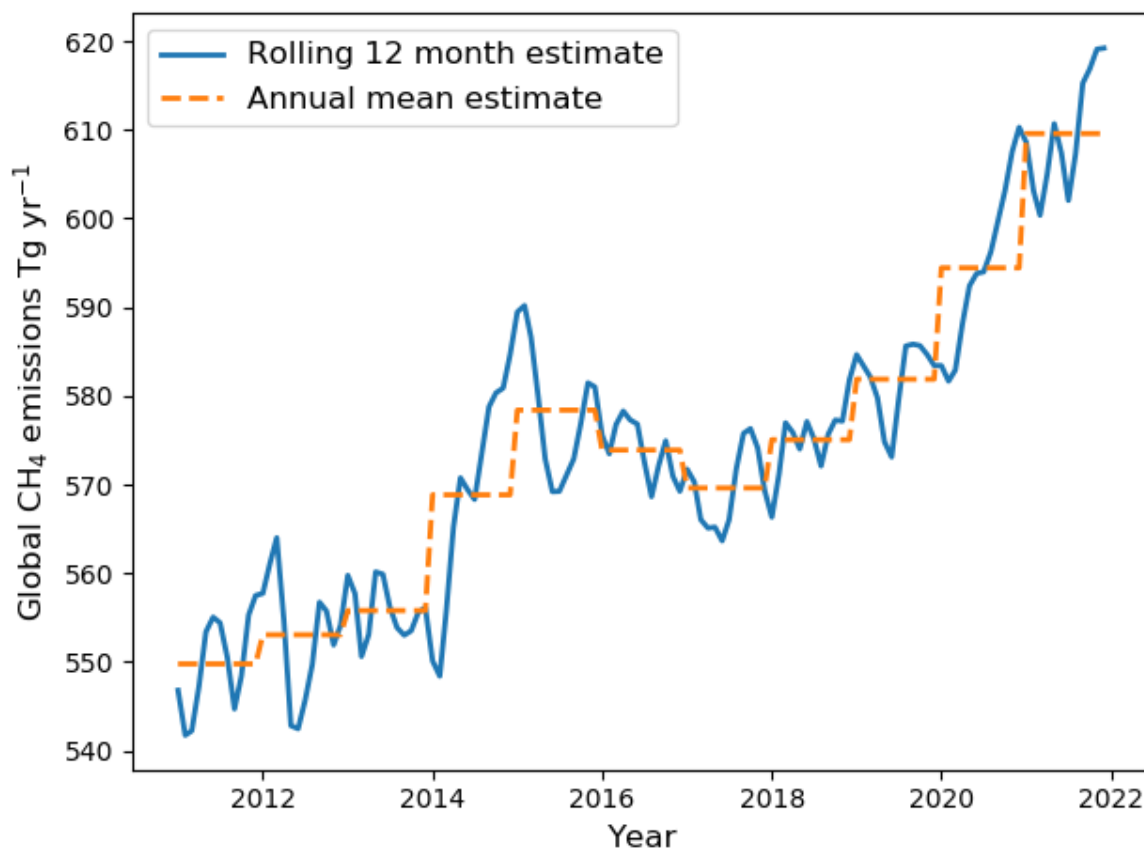
Figure B1 Global box model methane emission estimates between 2011 and 2021, respectively. Emission estimates are based on NOAA
410 global mean surface data. The blue line denotes the rolling 12-month annual emissions, and the orange line denotes the emissions based on
annual mean concentrations.

2-1

<u>Aug 5, 2022 at 3:00 PM, Reviewer</u>

By how much?

3-1

<u>Aug 5, 2022 at 3:00 PM, Reviewer</u>

For both CO2 and CH4, or just CH4?

3-2

<u>Jul 1, 2022 at 4:53 PM, Reviewer</u>

Olsen and Randerson is a downscaling technique. What biospheric model did you use?

3-3

<u>Aug 5, 2022 at 3:00 PM, Reviewer</u>

A 5% reduction is not that conservative. The spatial pattern of OH reduction is quite important. Miyazaki et al, 2021 (Science Advances) shows that the global mean reduction in OH is about 4%. However, the reductions can be substantially higher, (>30%) locally. These will directly affect the methane inferences, especially over Europe and parts of Asia.

Please review the paper and perform a sensitivity analysis closer to reported spatial changes in OH.

3-4

<u>Aug 5, 2022 at 3:00 PM, Reviewer</u>

We could expect, however, that the CO2 emission in 2020 and 2021 to be different than 2019. Not sure how this really addresses the OH issue.

As noted next, the Miyazaki et al, 2021 provides a more observationally constrained pattern of OH.

3-5

<u>Jul 1, 2022 at 4:53 PM, Reviewer</u>

Is this a correlation in flux or concentration space? If it is the former, where did 300km come from?

4-1

<u>Jul 1, 2022 at 4:53 PM, Reviewer</u>

You should be able to calculate the simulated atmospheric CH4 growth rate for 2020 and 2021 from your inversion. You should add that to the table (1).

The box-model approach carries its own assumptions, and can't be really used to validate the CH4 top-down estimates.

4-2

<u>Jul 1, 2022 at 4:53 PM, Reviewer</u>

Based upon NOx emission changes during 2020-2021, we would not expect CH4 lifetime to be fixed.

5-1

<u>Aug 5, 2022 at 3:00 PM, Reviewer</u>

There are no uncertainty estimates in this calculation. I can not assess whether these changes are statistically significant or not.

Uncertainty estimates need to be added to these flux estimates. These could be done through comparison with other inversions or independent observations.

5-2

<u>Jul 1, 2022 at 4:53 PM, Reviewer</u>

It looks like the increases in SA in 2021 are an acceleration of the 2020 increases. What is going on there?

5-3

<u>Jul 1, 2022 at 4:53 PM, Reviewer</u>

How is anomalous defined here? The temperature variations need to be calculated relative to the long term temperature variability to assess whether they are not within climatology.

5-4

<u>Jul 1, 2022 at 4:53 PM, Reviewer</u>

Please put plots of those regressions in the supplemental.

6-1 Aug 5, 2022 at 3:00 PM, Reviewer

Cooper didn't discuss NOx emissions, only concentrations. The impact on OH would need to be calculated separately and would be affected by other reactive species, e.g., ozone.

6-2 Jul 1, 2022 at 4:53 PM, Reviewer

It's hard to see the differences in a spatial plot. Please make a difference plot using the regions used in Fig. For 2020 and 2021 between the proxy retrieval and the simultaneous estimate.

6-3 Aug 5, 2022 at 3:00 PM, Reviewer

The implication of East Africa as the single largest driver of the methane growth rate is puzzling. Yes, there is a correlation with water anomalies, but it's not the largest driver of methane in driver.

A more plausible set of physical mechanisms needs to be proposed for why we could expect this region as a dominant driver.

7-1 Aug 5, 2022 at 3:00 PM, Reviewer

This is not clear to me at all that this is a valid assumption. The OH responses will depend on the regional NOx emission reductions and the timing of those reductions, in part because it will also affect ozone production. There are better sources for OH than this crude assumption.